Universität des Saarlandes

Fachrichtung 6.1 – Mathematik

Preprint

A Fourier transform based scheme for the Helmholtz equation

Mirjam Köhl

Preprint No. 73
Saarbrücken 2002

Universität des Saarlandes

Fachrichtung 6.1 – Mathematik

A Fourier transform based scheme for the Helmholtz equation

Mirjam Köhl

Saarland University
Department of Mathematics
Postfach 15 11 50
D–66041 Saarbrücken
Germany
E-Mail: koehl@num.uni-sb.de

submitted: October 25, 2002

Preprint No. 73

Saarbrücken 2002

Edited by
FR 6.1 – Mathematik
Im Stadtwald
D–66041 Saarbrücken
Germany

Fax: + 49 681 302 4443
e-mail: preprint@math.uni-sb.de
WWW: http://www.math.uni-sb.de/

Abstract

A new scheme based on the Fourier transform for the three-dimensional Helmholtz equation is introduced. We consider the boundary integral formulation for the Dirichlet boundary value problem and use the collocation boundary element method for the discretisation of the problem. In order to solve the resulting linear systems, the identity of the Fourier transform with respect to the wave number is applied to the associated matrices. We deduce the analytical forms and some important properties of the transformed matrices. Finally, some numerical examples for the solution are presented and we compare these with results using standard techniques.

AMS Subject Classification: 35J05, 65N38, 65R20
Keywords: Dirichlet problem, Helmholtz equation, single- and double-layer potential, Fourier transform, collocation

Contents

1 Introduction

We consider the exterior Dirichlet boundary value problem (BVP) for the three-dimensional Helmholtz equation (see e.g. [2])

$$\begin{aligned} \Delta u(x) + \kappa^2 u(x) &= 0\,, \qquad x \in \mathbb{R}^3 \setminus \bar{\Omega}\,, \quad \kappa = \frac{\omega}{c}\,, \\ u(x) &= g(x)\,, \quad x \in \Gamma\,. \end{aligned} \tag{1}$$

In (1), κ is the wave number which may be real or complex with $Im\,(\kappa) \geq 0$. $\Gamma = \partial\Omega$ denotes the smooth boundary of the bounded, connected domain Ω and $g(x)$ is a given function. To guarantee uniqueness of the solution $u(x)$, we add the Sommerfeld radiation conditions or outgoing wave conditions (cf. [8])

$$\Big(\frac{\partial}{\partial r} - i\kappa\Big) u(x) = o\,(\,|x|^{-1}) \text{ and } u(x) = O\,(\,|x|^{-1}) \quad \text{for large } |x| = r\,. \tag{2}$$

The Helmholtz equation arises in many physical problems related to wave propagation. In acoustic applications, ω and c are the frequency and velocity of the sound and u corresponds to the pressure field. We are interested in the solutions of (1) for a spectrum of (real) wave numbers $0 \leq \kappa \leq L$, where L is corresponding to the highest frequency. Boundary element methods (BEM) lead to a large linear system for each wave number. The memory requirement for such a problem is $Mem = O(N^2)$ and the numerical work using classical direct solvers is given by $Op = O(M\,N^3)$, where M denotes the number of frequencies and N is the number of degrees of freedom by BEM discretisation. Typical values are $N = 10^3 - 10^4$ for the dimension of the problem and $M = 10 - 10^2$ for the wave numbers of interest.
In this paper, we discuss a numerical method for the Helmholtz equation which is based on the Fourier transform with respect to the wave number κ. In particular, we examine in detail the case using the double-layer potential to treat the BVP (1) and summarize the properties of the single-layer potential representation of the solution which are described in our previous paper [7].

The paper is organised as follows.
In Section 2, we briefly review some basic properties of the Dirac δ-distribution and the Fourier transform. The exterior Dirichlet BVP is topic in Section 3. In particular, we describe the boundary integral formulation for the problem and its discrete forms. The new linear systems after applying the identity of the Fourier transform are discussed in Section 4. In Section 4.1, we

derive the analytical form of the transformed matrices and some important properties are given in Section 4.2. Finally, we present some numerical results (Section 5) and some conclusions (Section 6).

2 Preliminaries

For our subsequent applications, we introduce some basic definitions and properties corresponding to the Dirac δ-distribution and the Fourier transform. For more details, we refer the reader to [2], [4] and [6].

Let g be a real- or complex-valued function on $\mathbb{R}$.
The classical $\mathbb{L}_p$ spaces, $1 \leq p < \infty$, consists of functions g with the property

$$\mathbb{L}_p = \mathbb{L}_p(\mathbb{R}) = \{g : \mathbb{R} \to \mathbb{C} \text{ or } \mathbb{R}, \int_{\mathbb{R}} |g(x)|^p dx < \infty\}$$

and the corresponding norm is

$$\|g\|_{\mathbb{L}_p} = \left(\int_{\mathbb{R}} |g(x)|^p dx \right)^{\frac{1}{p}} .$$

The Schwartz space $\mathbb{S}$ of rapidly decreasing smooth test functions is defined by

$$\mathbb{S} = \mathbb{S}(\mathbb{R}) = \{g \in \mathbb{C}^\infty(\mathbb{R}) : |(1+x^2)^{\frac{m}{2}} g^{(n)}(x)| \leq C_{mn}\}$$

with arbitrary $m, n \in \mathbb{N}_o$, $x \in \mathbb{R}$ and some positive constants C_{mn}. Its adjoint space $\mathbb{S}'$ is called the space of tempered distributions.

2.1 Dirac δ-Distribution

Let $\psi : \mathbb{R} \to \mathbb{R}$ be a continuous function satisfying

$$\psi(x) = O\left(|x|^a\right), \quad |x| \to \infty$$

for some real a. Then ψ defines a real distribution over $\mathbb{S}$ by

$$< \psi, g >= \int_{\mathbb{R}} \psi(x) g(x) dx \quad \forall\, g \in \mathbb{S}\,. \tag{3}$$

Remark 1 *We will reserve the same notation* (3) *even for the Dirac* δ*-distribution. It holds* $\delta \in \mathbb{S}'$ *defined by*

$$< \delta\,,\, g >= g(0) \quad \forall\, g \in \mathbb{S}\,.$$

The derivation of a distribution ψ is well known as

$$< \psi',\, g >= - < \psi,\, g' > \ .$$

If we assume that $g(x) = a(x)\tilde{g}(x)$ with $a(x) \in \mathbb{C}^\infty(\mathbb{R})$, $g, \tilde{g} \in \mathbb{S}$, we obtain

$$< \psi',\, g >= - < \psi, a'\,\tilde{g} > - < \psi, a\,\tilde{g}' > \tag{4}$$

by applying the product rule.
In particular, the derivation of the Heaviside function $\mathbb{H}$ defined by

$$\mathbb{H}(x) = \begin{cases} 1\,, & x \geq 0 \\ 0\,, & x < 0 \end{cases}$$

is just the Dirac δ-distribution.

In our discussion, we will need an expression of the distribution $\delta(a(x))$, where $a(x)$ is differentiable and has n single zeros x_n.
In this case, we get

$$< \delta(a(x)), g >= \sum_n g(x_n) \frac{1}{|a'(x_n)|} \tag{5}$$

for all $g \in \mathbb{S}$.

2.2 Fourier Transform

For the complex-valued g, we define the one-dimensional Fourier transform by

$$\hat{g}(\kappa) \equiv \mathcal{F}_{\xi,\kappa}[g(\xi)](\kappa) = \int\limits_{\mathbb{R}} g(\xi) e^{i\kappa\xi} d\xi\,. \tag{6}$$

The corresponding inverse Fourier transform is then

$$g(\xi) = \mathcal{F}^{-1}_{\kappa,\xi}[\hat{g}(\kappa)](\xi) = \frac{1}{2\pi} \int\limits_{\mathbb{R}} \hat{g}(\kappa) e^{-i\kappa\xi} d\kappa\,, \tag{7}$$

from which we also have

$$\check{g}(\xi) \equiv \mathcal{F}^{-1}_{\kappa,\xi}[g](\xi) = \frac{1}{2\pi}\hat{g}(-\kappa) \quad \text{resp.} \quad \mathcal{F}_{\xi,\kappa}[\hat{g}](\kappa) = 2\pi g(-\kappa)\,. \tag{8}$$

The Fourier transform $\hat{g}$ exists, at least for $g \in \mathbb{L}_1$. In particular, (6) and (7) define the Fourier transform and its inverse for every test function $g \in \mathbb{S}$. It is well known that $\mathbb{S}$ is invariant under the Fourier transform and that under its inverse

$$\mathcal{F}^{\pm 1} : \mathbb{S} \to \mathbb{S}\,.$$

An important property of the Fourier transform is given by the Bessel-Parseval formula

$$< g, f >_{\mathbb{L}_2} = \int_{\mathbb{R}} g(\kappa)\overline{f(\kappa)}d\kappa = \frac{1}{2\pi} < \hat{g}, \hat{f} >_{\mathbb{L}_2} \quad \text{for all } f, g \in \mathbb{L}_2\,.$$

We notice that the Fourier transform of a tempered distribution $\psi \in \mathbb{S}'$ is defined by

$$< \psi,\, \hat{g} > = < \hat{\psi},\, g >$$

which holds for every test function $g \in \mathbb{S}$ and has the property

$$\mathcal{F}^{\pm 1} : \mathbb{S}' \to \mathbb{S}'\,.$$

Later, we will need the inverse Fourier transform of the constant 1.
Since the Fourier transform of the even Dirac δ-distribution is known

$$\hat{\delta} = 1\,,$$

we get, through (8),

$$\hat{1} = \hat{\hat{\delta}}(x) = \delta(x) \quad \text{and} \quad \check{1} = \delta(x)\,. \tag{9}$$

Another necessary application is the Fourier transform of a polynomial $P(\kappa)$ given by

$$\mathcal{F}_{\kappa,z}[P(\kappa)](z) = 2\pi P(-i\frac{d}{dz})\delta(z)\,. \tag{10}$$

3 The exterior Dirichlet BVP

In this section, we formulate boundary integral equations for the exterior Dirichlet BVP (1) and present its discrete forms using the point collocation method.

3.1 Boundary Integral Formulation

We introduce the acoustic single- and double-layer potentials

$$\begin{aligned} V_1(f)(y,\kappa) &= \int_\Gamma u^*(x,y,\kappa) f(x,\kappa)\, dF_x\,, \\ V_2(f)(y,\kappa) &= \int_\Gamma \frac{\partial\, u^*(x,y,\kappa)}{\partial\, n_x} f(x,\kappa)\, dF_x\,. \end{aligned} \tag{11}$$

for a given density function $f(\cdot,\kappa)$ defined on Γ and $y \in \mathbb{R}^3$. $u^*(x,y,\kappa)$ is the fundamental solution of the Helmholtz equation defined by

$$u^*(x,y,\kappa) = \frac{1}{4\pi}\frac{e^{i\kappa|x-y|}}{|x-y|}\,, \quad x,y \in \mathbb{R}^3.$$

Note that the fundamental solution and thus both potentials satisfy the Sommerfeld radiation conditions (2) (cf. [1]).

Using the double-layer potential V_2 in (11) to treat the Dirichlet BVP, we need to solve the boundary integral equation (BIE) for $y \in \Gamma$

$$\left(\frac{1}{2}\mathcal{I} + \mathcal{B}\right) f(y,\kappa) \equiv \frac{1}{2} f(y,\kappa) + \int_\Gamma \frac{\partial\, u^*(x,y,\kappa)}{\partial\, n_x} f(x,\kappa)\, dF_x = g(y,\kappa)\,. \tag{12}$$

We formulate

Theorem 2 *The exterior Dirichlet BVP*

$$\begin{aligned} &\Delta u(y) + \kappa^2 u(y) = 0 \qquad \text{for } y \in \Omega^c = \mathbb{R}^3 \setminus \bar{\Omega}\,, \\ &u(y) = g(y) \in H^r(\partial\Omega) \quad \text{for } y \in \partial\Omega\,, \quad r \in \mathbb{R}, \\ &u \text{ satisfies the radiation conditions (2)} \end{aligned} \tag{13}$$

has a unique solution

$$u(y) = \int_\Gamma \frac{\partial\, u^*(x,y,\kappa)}{\partial\, n_x} f(x,\kappa)\, dF_x \in H^{r+\frac{1}{2}}_{loc}(\Omega^c) \tag{14}$$

for all wave numbers κ. $f \in H^r(\partial\Omega)$ denotes the solution of the BIE (12).

If $-\kappa^2$ is not an eigenvalue of the interior Neumann BVP for the Laplacian, then the BIE is uniquely solvable. Otherwise the kernel of $\frac{1}{2}\mathcal{I} + \mathcal{B}$ becomes nontrivial.

Similary, we can use the single-layer potential V_1 and get the BIE for $y \in \Gamma$

$$\mathcal{A}f(y,\kappa) \equiv \int_\Gamma u^*(x,y,\kappa) f(x,\kappa)\, dF_x = g(y,\kappa)\,. \tag{15}$$

The uniqueness of the solution is given by the

Theorem 3 *The exterior Dirichlet BVP* (13) *with* $g \in H^{r+1}(\partial\Omega)$ *has a unique solution*

$$u(y) = \int_\Gamma u^*(x,y,\kappa) f(x,\kappa)\, dF_x \in H^{r+\frac{3}{2}}_{loc}(\Omega^c)$$

for a unique $f \in H^r(\partial\Omega)$ *solving the BIE* (15)*, provided* $-\kappa^2$ *is not an eigenvalue of the interior Dirichlet BVP for the Laplacian.*

Remark 4 *If* $-\kappa^2$ *is an eigenvalue of the interior Dirichlet BVP for the Laplacian, then the BIE* (15) *is solvable, if and only if* g *is orthogonal to the cokernel (=kernel) of* $\mathcal{A}$*. In this case, the solution* f *is not unique, cf. [3].*

Throughout the rest of this discussion, we assume that the equation (15) is solvable.

It should be remarked that the operators for the corresponding interior Dirichlet BVP are given by respective $-\frac{1}{2}\mathcal{I} + \mathcal{B}$ and $\mathcal{A}$. In these cases, the solutions f of the associated BIE are unique, provided $-\kappa^2$ is not an eigenvalue of the interior Dirichlet BVP for the Laplacian.

For more details and the proofs of the theorems, we refer the readers to [2] or [3].

3.2 Collocation Method

Let the surface Γ be discretised using a system of plane, triangle panels

$$\Gamma \approx \Gamma_h = \bigcup_{j=1}^{N} \Gamma_j\,.$$

Since the unknown function $f(x,\kappa)$ depends on $x \in \Gamma$ and the wave number κ, we devide the approximate function f_h in a product

$$f_h(x,\kappa) = \sum_{j=1}^{N} \alpha_j(\kappa)\varphi_j(x)$$

where φ_j, $j = 1, \ldots, N$, are the associated ansatz functions.

Therefore, the BIE (12) leads to

$$\left(\frac{I}{2} + B(\kappa)\right) \alpha(\kappa) = \varrho(\kappa)\,,\ B \in \mathbb{C}^{N\times N}\,,\ \alpha,\ \varrho \in \mathbb{C}^N\,. \tag{16}$$

The elements of the matrix B are defined by

$$b_{ij}(\kappa) = \frac{1}{4\pi} \int_\Gamma \frac{\partial}{\partial n_x} \frac{e^{i\kappa|x-y_i|}}{|x-y_i|} \varphi_j(x) dF_x\,,$$

where y_i, $i = 1, \ldots, N$, denote the corresponding collocation points.
Using

$$\frac{\partial}{\partial n_x} \frac{e^{i\kappa|x-y_i|}}{|x-y_i|} = \frac{e^{i\kappa|x-y_i|}}{|x-y_i|^3} \left(i\kappa|x-y_i| - 1\right) < n_x, x-y_i >\,,$$

the expression above can be rewritten in the form

$$b_{ij}(\kappa) = \frac{1}{4\pi} \int_\Gamma \frac{e^{i\kappa|x-y_i|}}{|x-y_i|^3} \left(i\kappa|x-y_i| - 1\right) < n_x, x-y_i > \varphi_j(x) dF_x\,.$$

If the BIE corresponds to the single-layer representation (15), we get

$$A(\kappa)\alpha(\kappa) = \varrho(\kappa)\,,\ A \in \mathbb{C}^{N\times N}\,,\ \alpha,\ \varrho \in \mathbb{C}^N \tag{17}$$

where

$$a_{ij}(\kappa) = \frac{1}{4\pi} \int_\Gamma \frac{e^{i\kappa|x-y_i|}}{|x-y_i|} \varphi_j(x) dF_x$$

are the entries of the matrix A.
In both cases, the vector α and the right-hand side of the systems are given by

$$(\alpha(\kappa))_j = \alpha_j(\kappa) \text{ and } (\varrho(\kappa))_i = g(y_i, \kappa)\,, \quad i, j = 1, \ldots, N\,.$$

Remark 5 *The equations* (16) *and* (17) *explicitly depend on the wave number* κ.

Throughout the rest of the discussion, we assume that $\kappa \in \mathbb{R}^+$.

4 Linear Systems

In order to solve the system of linear equations, we apply the identity of the Fourier transform with respect to the wave number κ to the collocation matrices

$$C(\kappa) = \mathcal{F}_{\xi,\kappa}\left[\mathcal{F}^{-1}_{\kappa,\xi}\left[\,C(\kappa)\,\right](\xi)\right](\kappa)\,,$$

with respectively $C = B$ and $C = A$.

4.1 Transformed Matrices

The entries of the matrix $\check{B}(\xi) = \mathcal{F}^{-1}_{\kappa,\xi}\left[\,B(\kappa)\,\right](\xi)$ are given by

$$\check{b}_{ij}(\xi) = \frac{1}{4\pi}\int\limits_{\Gamma}\frac{1}{r^3}\left(r\frac{d}{dz}-1\right)\delta(z)\Big|_{z=r-\xi} < n_x, x-y_i > \varphi_j(x)dF_x\,. \qquad (18)$$

with $r = |x-y_i|$ as a consequence of

$$\mathcal{F}^{-1}_{\kappa,\xi}[e^{i\kappa r}\,(i\kappa r-1)](\xi) = \frac{1}{2\pi}\mathcal{F}_{\kappa,z}[i\kappa r-1](z)\big|_{z=r-\xi}$$

and (10).

Remark 6 *The distribution $\delta(z)$, $z = |x-y_i|-\xi$, is concentrated on a ball of radius ξ centred at y_i. Due to its definition, the integration domain leads to integration over the intersection of Γ and the surface of this ball.*
Further, ξ can be restricted to $[\,0, diam(\Gamma)\,]$ where $diam(\Gamma) = \sup\limits_{x,y\in\Gamma}|x-y|$.

Since we assume that Γ_j, $j = 1,\ldots,N$, are plane triangles and the ansatz functions are piecewise constant on Γ_j, i.e.

$$\varphi_j(x) = \begin{cases} 1 \text{ on } \Gamma_j \\ 0 \text{ otherwise,} \end{cases}$$

then the centres of the mass of the panels Γ_i build a system of collocation points

$$y_i = \frac{1}{3}\Big(x_i^{(1)} + x_i^{(2)} + x_i^{(3)}\Big)\,, \quad i = 1,\ldots,N\,.$$

In this situation, the elements of the matrix $\check{B}(\xi)$ can be computed analytically as follows.
Let us denote the projection of the point y_i into the plane of the triangle Γ_j with y_i', $y_i' = y_i - d\cdot n_x$. First, we rotate and translate the system of

coordinates in such a way that the origin coincides with the point y_i', the e_1-axis is directed along a side of the triangle, especially the side $x_j^{(1)}x_j^{(2)}$, and the e_3-axis is directed along the unit normal vector n_x.

In these new coordinates, a point $x \in \Gamma_j$ takes the form

$$x' = Q(x - y_i') = (x_1', x_2', 0)\,,$$

where Q denotes the corresponding rotation matrix. Further, the scalar product in (18) is given by

$$< n_x, x - y_i >= \begin{cases} 0 \text{ for } i = j \\ -d \text{ otherwise.} \end{cases} .$$

Figure 1 illustrates the situation described.

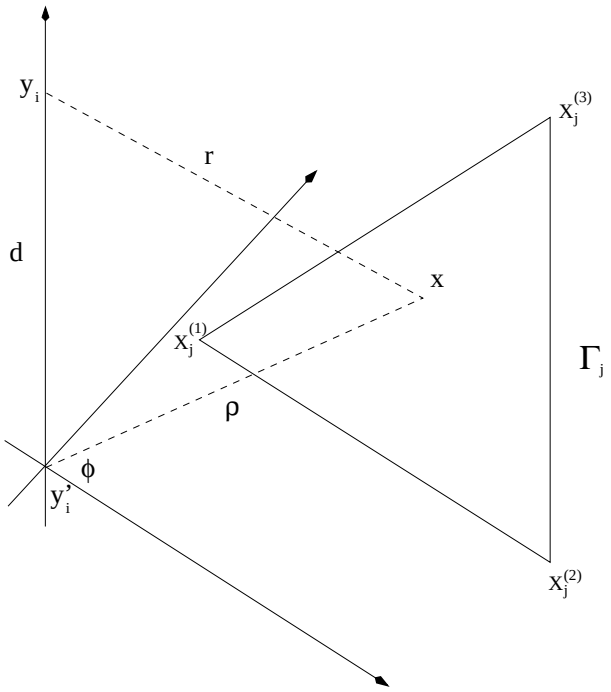

Figure 1: Computation of the elements of the matrices

The integral (18) will be evaluated in polar coordinates in the plane of the triangle Γ_j. Using the notation from Figure 1 and noting the relation $\rho d\rho = r dr = (z + \xi)dz$, we obtain for $i \neq j$

$$
\begin{aligned}
\check{b}_{ij}(\xi) &= \frac{-d}{4\pi}\int_{\Phi_1}^{\Phi_2}\int_{z_{min}}^{z_{max}}\left(\frac{\delta'(z)}{(z+\xi)}-\frac{\delta(z)}{(z+\xi)^2}\right)dzd\phi \\
&\overset{(4)}{=} \frac{1}{4\pi}\frac{d}{\xi}\int_{\Phi_1}^{\Phi_2}(\mathbb{1}'_{[z_{min},z_{max}]}(z))\big|_{z=0}\,d\phi \\
&= \frac{1}{4\pi}\frac{d}{\xi}\int_{\Phi_1}^{\Phi_2}\delta(-z_{min}(\phi))-\delta(-z_{max}(\phi))d\phi\,, \qquad (19)
\end{aligned}
$$

through $\mathbb{1}_{[z_{min},z_{max}]}(z) = \mathbb{H}(z-z_{min}) - \mathbb{H}(z-z_{max})$ and $\mathbb{H}'(z) = \delta(z)$.

In order to compute the integral (19), we first consider the situation described in the following Figure.

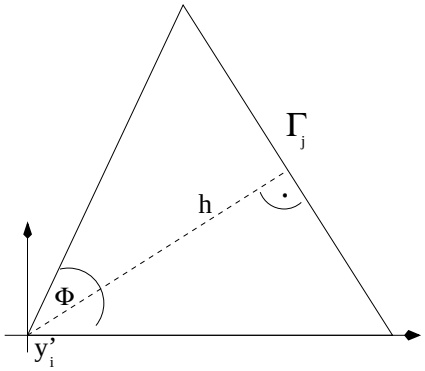

Figure 2: y_i' coincides with one of the edges of the triangle Γ_j

In this case, we formulate

Theorem 7 *The elements of the matrix $\check{B}(\xi) \in \mathbb{R}^{N\times N}$ are given by*

$$
\check{b}_{ij}(\xi) = \begin{cases} 0\,, & i=j \\ \dfrac{\Phi}{4\pi}\dfrac{d}{\xi}\,\delta(\xi-|d|) - \dfrac{1}{4\pi}\beta_{ij}(\xi) \end{cases} \qquad (20)
$$

where

$$
\beta_{ij}(\xi) = \frac{d}{\xi^2-d^2}\frac{h}{\sqrt{\xi^2-d^2-h^2}}\mathbb{1}_{[\xi_{min},\xi_{max}]}(\xi)\,.
$$

It holds $\xi_{min} \geq \xi_o = \sqrt{d^2+h^2}$ and h denotes the minimal distance of a side of the triangle and the origin (c.f. Figure 2).

Proof. We consider the entries in the form (19) with $\Phi_1 = 0$ and $\Phi_2 = \Phi$. The relation (5) and the fact that $z_{min}(\phi) = |d| - \xi$ is independent of ϕ lead to

$$\check{b}_{ij}(\xi) = \frac{1}{4\pi}\frac{d}{\xi}\,\Phi\,\delta(\xi - |d|) - \frac{1}{4\pi}\frac{d}{\xi}\sum_n \frac{\mathbb{1}_{[0,\Phi]}(\phi_n)}{|(-z'_{max}(\phi))_{|\phi=\phi_n}|}\,.$$

The expression (20) follows after short calculations using the relation

$$|(-z'(\phi))_{|\phi=\phi_o}| = \frac{\xi^2 - d^2}{\xi}\frac{\sqrt{\xi^2 - d^2 - h^2}}{h}$$

for any zero of the function $z(\phi)$. ∎

The expression (20) implies that each element $\check{b}_{ij}(\xi)$ has a local support. Therefore the matrix $\check{B}(\xi)$ has a sparse structure for a fixed ξ. It should be remarked that $\beta_{ij}(\xi)$ becomes singular at the point $\xi = \xi_0$.

If the projection y'_i does not coincide with one of the edges, then we can always reduce the calculation of the integral to calculating three integrals of the previous type. Thus, the analytical computation of the entries $\check{b}_{ij}(\xi)$ is given in any case.

Throughout the rest of the discussion, we assume the expression (20) from Theorem 7.

In a similar manner, we get the inverse Fourier transform of the matrix $A(\kappa)$ by

$$\check{a}_{ij}(\xi) = \frac{1}{4\pi}\frac{1}{\xi}\int_\Gamma \delta(\xi - |x - y_i|)\varphi_j(x)dF_x\,,$$

since

$$\mathcal{F}^{-1}_{\kappa,\xi}[e^{i\kappa|x-y_i|}](\xi) = \mathcal{F}^{-1}_{\kappa,\xi}[1](\xi - |x - y_i|)$$

and applying (9).
Transforming the geometry as described above and using the notation from Figure 1, we obtain for all $i, j = 1, \ldots, N$

$$\begin{aligned}\check{a}_{ij}(\xi) &= \frac{1}{4\pi}\frac{1}{\xi}\int_{\Phi_1}^{\Phi_2}\int_d^{r_{max}} \delta(\xi - r)r\,dr\,d\phi \\ &= \frac{1}{4\pi}\left(\Phi_2(\xi) - \Phi_1(\xi)\right)\,. \qquad (21)\end{aligned}$$

The matrix $\check{A}(\xi)$ is also real and sparse for a fixed ξ, because each element $\check{a}_{ij}(\xi)$ has a local support, $\mathrm{supp}[\,\check{a}_{ij}\,] = [\xi^*_{min}, \xi^*_{max}\,]$, cf. Remark 6.

4.2 New Linear Systems

After studying the inverse transformed matrices, we return to matrices which depend on the wave number κ.
Applying the Fourier transform to the matrix $\check{B}(\xi)$, we obtain for the term $\beta_{ij}(\xi)$ in (20)

$$\left(\mathcal{F}_{\xi,\kappa}\left[\beta_{ij}(\xi)\right](\kappa)\right) \;=\; e^{i\kappa\xi_o}\int\limits_{\xi_{min}}^{\xi_{max}} \beta_{ij}(\xi)d\xi \;+\; \int\limits_{\xi_{min}}^{\xi_{max}} \beta_{ij}(\xi)\left(e^{i\kappa\xi} - e^{i\kappa\xi_o}\right)d\xi \quad (22)$$

Since the analytical computation of

$$\int\limits_{\xi_{min}}^{\xi_{max}} \beta_{ij}(\xi)d\xi = \gamma_{ij}(\xi)\Big|_{\xi_{min}}^{\xi_{max}}$$

with

$$\gamma_{ij}(\xi) = \begin{cases} 0 \text{ for } \xi = \xi_0 \\ \dfrac{1}{2}\left(\arctan\left(\dfrac{\xi_0^2 + d\xi}{h\sqrt{\xi^2 - \xi_0^2}}\right) - \arctan\left(\dfrac{\xi_0^2 - d\xi}{h\sqrt{\xi^2 - \xi_0^2}}\right)\right) \end{cases}$$

is independent of the wave number, we need to estimate the first integral in (22) once. A further property is the smoothness of the second integrant. Using the Gaussian formula for the approximation, it holds

$$\int\limits_{\xi_{min}}^{\xi_{max}} \beta_{ij}(\xi)\left(e^{i\kappa\xi} - e^{i\kappa\xi_0}\right)d\xi \;\;\approx\;\; i\kappa e^{i\kappa\xi_0} h_\xi \sum_{k=1}^{m} w_k \bar{\beta}_{ij}(\xi_k)\mathrm{sinc}(\kappa\xi_k)e^{i\kappa\xi_k}$$

where $\bar{\beta}_{ij}(\xi) = \xi\,\beta_{ij}(2(\xi + \xi_0))$ is also independent of κ and the relevant parameters are given by

$$\xi_k = \bar{\xi} + h_\xi x_k\,, \quad h_\xi = \frac{\xi_{max} - \xi_{min}}{4} \text{ and } \bar{\xi} = \frac{\xi_{max} + \xi_{min} - 2\xi_0}{4}\,.$$

x_k denote the zeros of the Legendre polynomials P_m of order m and w_k are the associated weights.

Due to the definition of $\delta(\xi - |d|)$, the system of linear equations (16) leads to

$$\frac{1}{2}\alpha(\kappa) + \tilde{B}(\kappa)\alpha(\kappa) = \varrho(\kappa) \tag{23}$$

where the entries of the matrix $\tilde{B}(\kappa)$ are given by

$$\begin{aligned} \tilde{b}_{ii}(\kappa) &= 0 \\ \tilde{b}_{ij}(\kappa) &= \frac{\Phi}{4\pi}\,\mathrm{sgn}(d)\, e^{i\kappa|d|} \\ &\quad -\frac{e^{i\kappa\xi_0}}{4\pi}\left(\gamma_{ij}(\xi)\Big|_{\xi_{min}}^{\xi_{max}} + i\kappa h_\xi \sum_{k=1}^{m} w_k \bar{\beta}_{ij}(\xi_k)\mathrm{sinc}(\kappa\xi_k)e^{i\kappa\xi_k}\right). \end{aligned} \tag{24}$$

The elements of the matrix $\check{A}(\xi)$ will be transformed as follows.
After restricting the integration domain to its support, we approximate the function $\check{a}_{ij}(\xi)$ inside this interval using n piecewise constant splines

$$\int_{\xi^*_{min}}^{\xi^*_{max}} \check{a}_{ij}(\xi)e^{i\kappa\xi}d\xi \approx h_\xi \sum_{l=0}^{n-1} \check{a}_{ij}(l) \int_{l}^{l+1} e^{i\kappa(\xi^*_{min}+th_\xi)}dt$$

where

$$\check{a}_{ij}(l) = \int_{l}^{l+1} \check{a}_{ij}(\xi^*_{min} + th_\xi)dt \quad \text{and} \quad h_\xi = \frac{\xi^*_{max} - \xi^*_{min}}{n},\ n \in \mathbb{N}.$$

Since the integral term will be computed analytically, we also get a linear system

$$\tilde{A}(\kappa)\alpha(\kappa) = \varrho(\kappa) \tag{25}$$

with a new collocation matrix depending on κ

$$\tilde{a}_{ij}(\kappa) = h_\xi\, e^{i\kappa(\xi^*_{min}+\frac{h_\xi}{2})}\,\mathrm{sinc}\left(\frac{\kappa h_\xi}{2}\right)\sum_{l=0}^{n-1}\check{a}_{ij}(l)e^{i\kappa l h_\xi}\,. \tag{26}$$

Notice that the term outside of the sum depends only on the wave number and will be evaluated separately.

Remark 8 *Due to the independence of the wave number κ, the values $\gamma_{ij}(\xi)$ and $\bar{\beta}_{ij}(\xi)$ in* (24) *and, similary, $\check{a}_{ij}(l)$ in* (26) *need to be calculated only once. Thus we will treat the respective linear systems* (23) *and* (25) *for several $\kappa \le L$ using always these computed data.*

5 Numerical Results

We present numerical experiments for the boundary integral formulation

$$\mathcal{A}v = \left(\frac{1}{2}\mathcal{I} + \mathcal{B}\right) f \quad \text{and} \quad \mathcal{A}v = \left(-\frac{1}{2}\mathcal{I} + \mathcal{B}\right) f \tag{27}$$

for the respective interior and exterior Dirichlet BVPs for the Helmholtz equation using collocation with piecewise constant ansatz functions.
In (27), $\mathcal{A}$ and $\mathcal{B}$ denote the single-layer and double-layer potentials of the Helmholtz equation. Since we chose

$$f = u^*(x, y_0, \kappa) = \frac{1}{4\pi}\frac{e^{i\kappa|x-y_0|}}{|x-y_0|}, \quad x \in \Gamma,$$

$y_0 \notin \overline{\Omega}$ for the interior and $y_0 \in \Omega$ for the exterior problem, the solution of the equation (27) is known to be $v = \partial_{n_x} u^*(x, y_0, \kappa)|_{x\in\Gamma}$.

Here, all numerical tests are performed for the surface of the unit sphere

$$\Gamma = \{x \in \mathbb{R}^3, |x| = 1\},$$

approximated using a system of $N = 1280$ plane, triangle panels. We are interested in a spectrum of $M = 200$ wave numbers bounded by $L = 8$.

In order to study the behaviour of the solutions v_{FT} which arise from the so called Fourier method described in Section 4, we compare these and the results using standard techniques v_{ST} with the analytical solutions v. Note that "using standard techniques" means the use of numerical integration for the computation of the matrices.
In the graphs below, the solution v_{FT} is highlighted in black, v_{ST} is pointed and the dashed line corresponds to the analytical solution.

Figure 3 shows the error of the solutions in the $\mathbb{L}_2$ norm. The error of the solution using standard techniques increases with a larger wave number, while the error v_{FT} is almost constant apart from some discrete peaks. These result from the fact that the negative square of these wave numbers are exactly the eigenvalues of the Laplacian on the unit sphere, cf. the relevant theorems and remarks in Section 3.1.

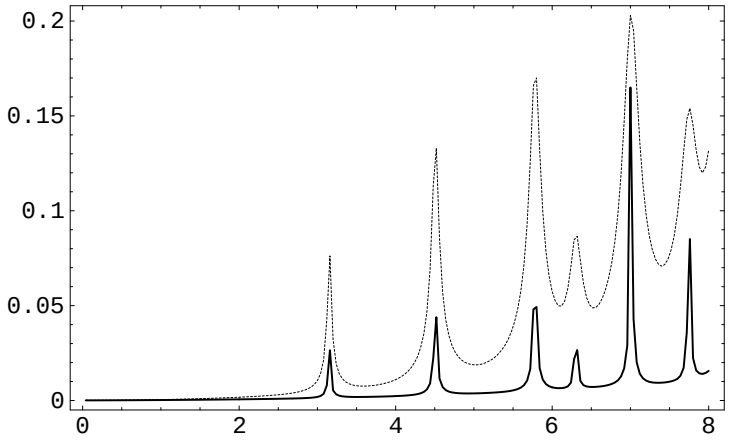

a) Interior Problem

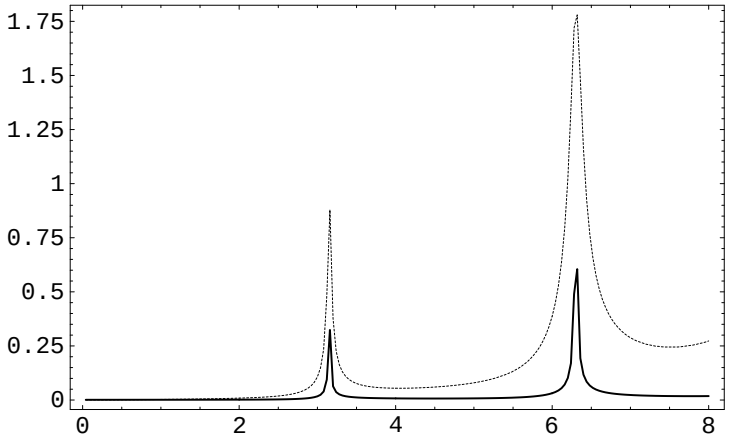

b) Exterior Problem

Figure 3: $\mathbb{L}_2$ error of the solutions in dependence on the wave number

Next, we selected one component of the solutions and printed it depending on the wave number κ, see Figure 4 and 5. In all cases, we decide that the results of the Fourier method correspond well with the analytical values. Only for the eigenvalues it differs a bit. The curves of the solution v_{ST} differ increasingly for larger wave numbers.

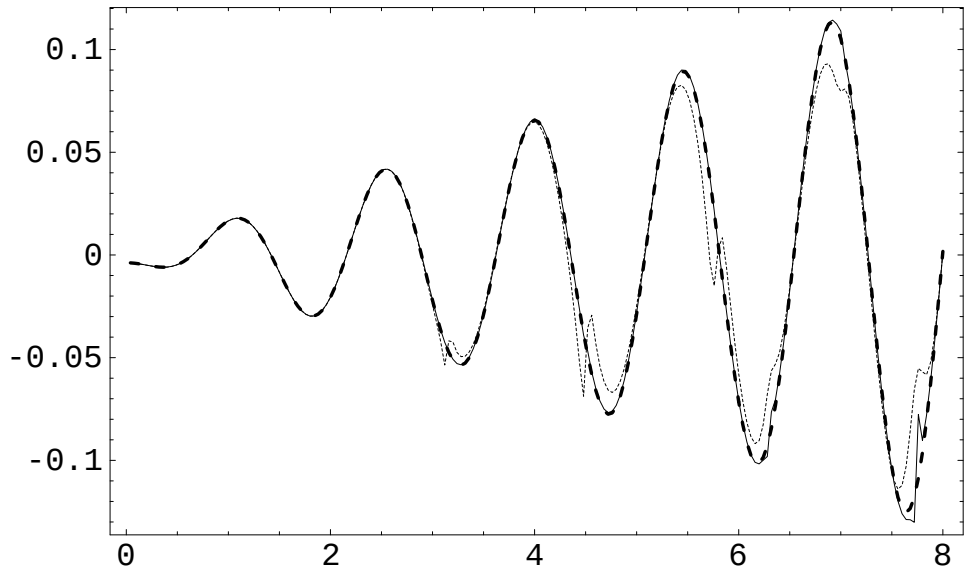

a) Real Part

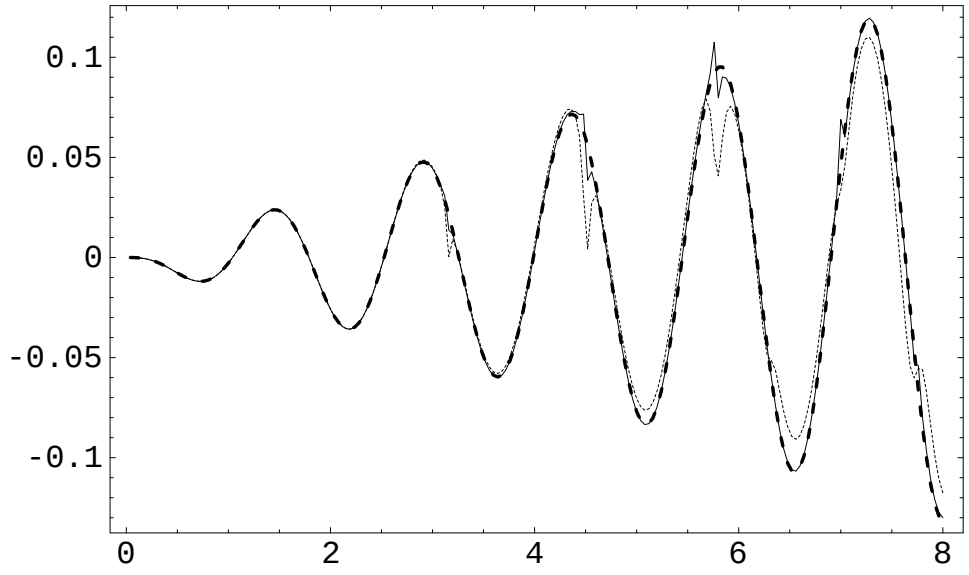

b) Imaginary Part

Figure 4: The course of the solutions in dependence on the wave number - Interior problem

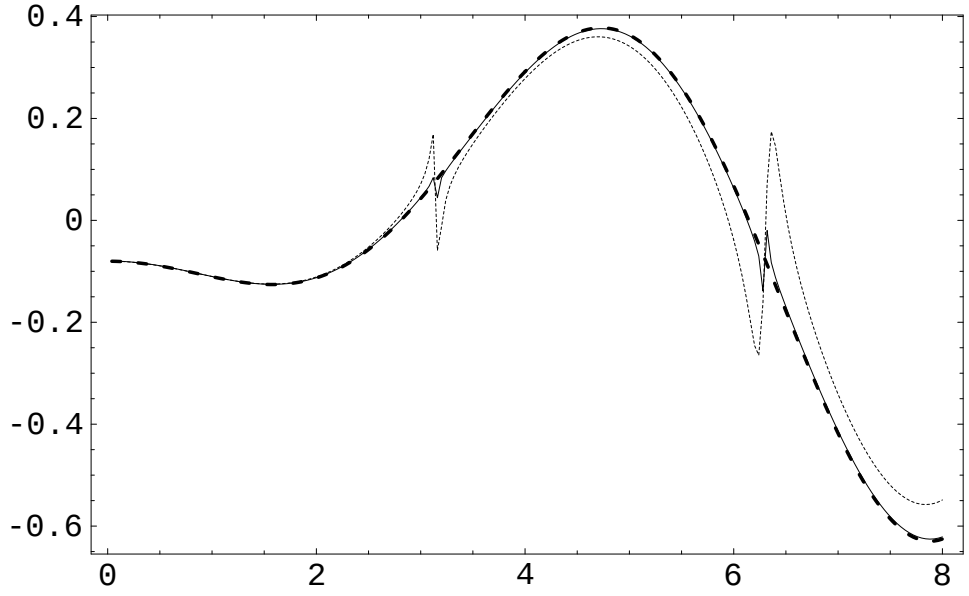

a) Real Part

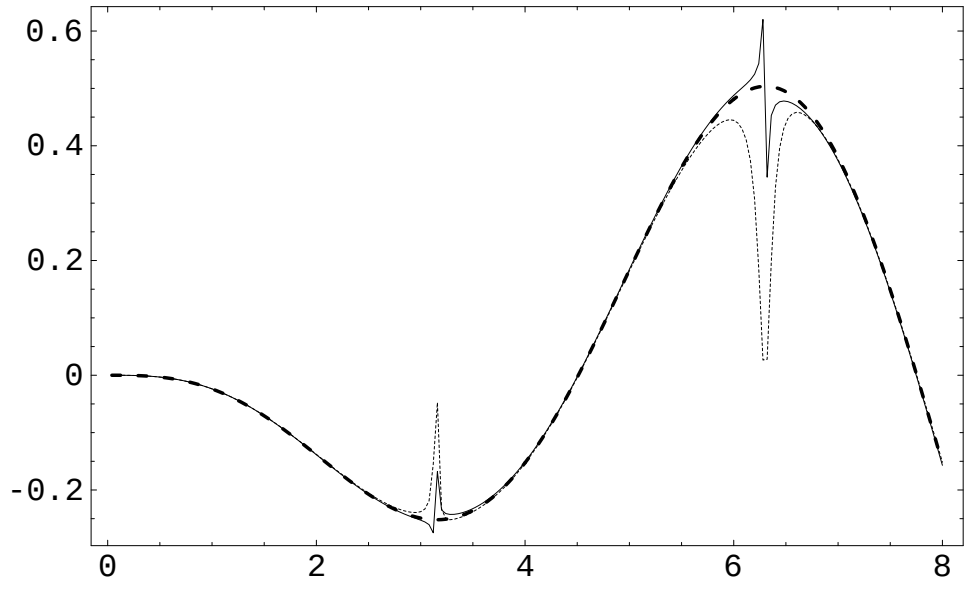

b) Imaginary Part

Figure 5: The course of the solutions in dependence on the wave number - Exterior problem

In order to examine the behaviour of the solutions v_{FT} in dependence on the dimension N, we differentiate between the behaviour of the error for $\kappa h = const.$ and the convergence for a fixed wave number κ with the discretisation parameter h tending to 0, cf. [5].

Table 1 shows the behaviour of the errors for various wave numbers satisfying the condition $\kappa h \approx 0.7$.
We decide that the deviation of the solution of the interior problem results from the fact that the wave number $\kappa = 7.84$ lies close to an eigenvalue of the Laplacian (see also Figure 3).

Table 1: $\mathbb{L}_2$ error of the solutions for various κ with $\kappa h \approx 0.7$

N	κ	κh	$\|\|v^* - v_{FT}\|\|_{\mathbb{L}_2}$ (interior)	$\|\|v^* - v_{FT}\|\|_{\mathbb{L}_2}$ (exterior)
20	1.15	0.698	0.795E-02	0.517E-01
80	2.04	0.697	0.708E-02	0.145E-01
320	3.94	0.699	0.760E-02	0.224E-01
1280	7.84	0.702	0.159E-01	0.179E-01

In Table 2, the convergence of the solutions v_{FT} of the respective interior and exterior problems is printed for $\kappa = \pi/2$.

Table 2: Convergence of the solutions for $\kappa = \pi/2$

N	κh	$\|\|v^* - v_{FT}\|\|_{\mathbb{L}_2}$ (interior)	$\|\|v^* - v_{FT}\|\|_{\mathbb{L}_2}$ (exterior)
20	0.953	0.112E-01	0.532E-01
80	0.538	0.473E-02	0.134E-01
320	0.278	0.143E-02	0.380E-02
1280	0.140	0.418E-03	0.146E-02

It should be pointed out that the new scheme uses only half of the computing time compared to the case using standard techniques.

6 Conclusions

In this paper, we presented a new Fourier method for the Helmholtz equation, in particular for the exterior Dirichlet BVP. The transformed collocation ma-

trices, which are real and have sparse structures, were discussed. We pointed out the advantages of solving the new resulting linear systems. Numerical tests of the new sheme show the good agreement of the boundary element results with the analytical solutions.

In a similar manner, we can apply the described Fourier method to the Neumann or impedance BVP for the Helmholtz equation.

References

[1] C. A. Brebbia, J.C.F. Telles, and L.C. Wrobel, editors. *Boundary element techniques.* Springer-Verlag, Berlin, 1984. Theory and applications in engineering.

[2] G. Chen and J. Zhou. *Boundary element methods.* Academic Press Ltd., London, 1992.

[3] D. L. Colton and R. Kress. *Integral equation methods in scattering theory.* Krieger Publishing Company, Malabar, 1992.

[4] I. M. Gelfand and G. E. Schilow. *Verallgemeinerte Funktionen (Distributionen). I: Verallgemeinerte Funktionen und das Rechnen mit ihnen.* Hochschulbücher für Mathematik, Bd. 47. VEB Deutscher Verlag der Wissenschaften, Berlin, 1960.

[5] K. Giebermann. *Schnelle Summationsverfahren zur numerischen Lösung von Integralgleichungen für Streuprobleme im R^3.* Dissertation, Universität Karlsruhe, 1997.

[6] L. Hoermander. *The analysis of linear partial differential operators, I.* Springer-Verlag, Berlin, second edition, 1990. Distribution theory and Fourier analysis.

[7] M. Köhl and S. Rjasanow. *Multifrequency Analysis for the Helmholtz Equation.* Preprint 64, 2002. to appear in IABEM 2002 issue of Computational Mechanics, Springer.

[8] J.-C. Nédélec. *Acoustic and electromagnetic equations.* Springer-Verlag, New York, 2001. Integral representations for harmonic problems.